

RESEARCH ARTICLE | FEBRUARY 21 2019

Stress analysis of a strip under tension with a circular hole

FREE

Ireneusz Kozera; Violetta Konopińska-Zmysłowska; Marcin Kujawa ✉



AIP Conf. Proc. 2077, 020028 (2019)

<https://doi.org/10.1063/1.5091889>



View
Online



Export
Citation

CrossMark

AIP Advances

Why Publish With Us?

- 25 DAYS**
average time to 1st decision
- 740+ DOWNLOADS**
average per article
- INCLUSIVE**
scope

[Learn More](#)

Stress Analysis of a Strip Under Tension with a Circular Hole

Ireneusz Kozera¹, Violetta Konopińska-Zmysłowska¹ and Marcin Kujawa^{1, a)}

¹*Gdansk University of Technology, Faculty of Civil and Environmental Engineering, 80-233 Gdańsk, ul. G. Narutowicza 11/12, Poland*

^{a)}Corresponding author: mark@pg.edu.pl

Abstract. The paper addresses stress analysis of a strip with a circular hole under uniform uniaxial tension based on circumferential stress expression σ_θ . Stresses are analyzed in the infinite-length strips under tension with holes, the ratio of the hole radius a to the strip half-width b is either equal to: $\lambda = a/b = 0.1$ or $\lambda = 0.5$. Circumferential stresses are determined in selected cross-sections of the strip. The stress diagrams display local stress concentration near the hole. The analytical solutions are compared with the numerical solutions the finite elements method (FEM), the latter using the ABAQUS software due to various λ ratios. The results show the maximum circumferential stress at hole boundary, affected by the ratio of the hole radius to the width of the strip.

The work was created as part of B.Sc. engineering thesis at Gdansk University of Technology, Faculty of Civil and Environmental Engineering.

INTRODUCTION

Stress concentration problems are significant in structural mechanics, thus widely considered and analysed in literature. The present day technical and scientific literature often regards stress concentration problems in plates and shells. It proves validity of problem and challenge in searching for solutions. Three-dimensional solution for the stress field around a circular hole in a plate far-field tension is presented in [1]. Stress concentration factor of a plate with a circular hole under tension is analysed in the work [2] by means of the finite element method. Numerical methods to deal with stress concentration in isotropic plates with discontinuities are included in the paper [3]. The article [4] analyses an isotropic plate with a noncircular hole under uniform tension. Stress concentration in finite metallic plates with regular holes under uniaxial loading is considered in [5]. In the paper [6] elastic stress and strain fields of plates with a single central hole and two auxiliary holes subjected to uniaxial tension are investigated by means of the finite element method. The FEM-based analysis of plates with holes of different shapes: circular, square and rectangular are analysed in [7]. In [8] the authors present geometric elasticity problem of stress concentration in a plate with a circular hole under uniaxial tension, biaxial tension and shear. Theoretical solution of a rectangular plate with an arbitrarily located circular hole subjected to in-plane bending moment is presented in [9]. Interaction between two neighbouring circular holes in an orthotropic strip subjected to bending is considered in [10]. In [11] the authors analyse stress concentration in an elastic square plate with a full-strength hole under bending. The 3D FEM-based analysis of the stress and strain concentration in an elastic plate of finite thickness with a circular hole subjected to tension is included in the papers [12], [13]. The elliptical hole core is considered in [14], two interacting holes are investigated in [15]. Shape optimization of a hole in an orthotropic plate at the biaxial compression is presented in [16]. The stress concentration problem is also important in shell structures, e.g. in [17] stresses are analysed around holes in cylindrical parts of prestressed concrete protective shells. Simplified stress distributions in plate with circular hole under uniform tension can be found in the works [18], [19]. Other stress distribution functions around holes in plates and girders are included in [20], [21].

The paper concerns stress analysis of a strip under tension with a circular hole and considers the plane stress continuous theory of elasticity, addressed in [22]. In the work three well-known approaches are compared: the



analytical ones, proposed by Girkmann [18] and Howland [20] and the FEM-based numerical solution. Sufficient accuracy of the results is observed within the scope of the stated assumptions.

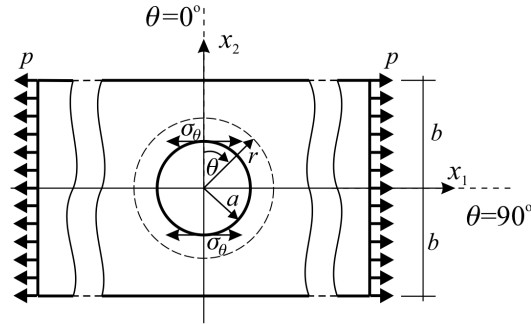


FIGURE 1. Static diagram.

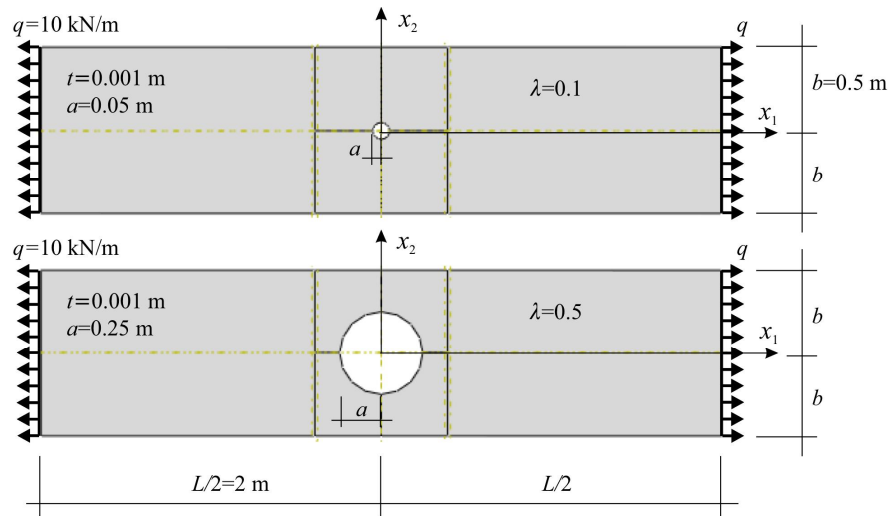


FIGURE 2. Numerical examples – data.

PLANE STRESS

The paper is focused on structural analysis of plates. The structure is analysed in plane stress assuming that the in-plane loads act only, the stress components perpendicular to the plate are zero. Thus stresses in the system are presented in the form of a symmetric two-dimensional Cauchy tensor consisting of three independent components: σ_{11} , σ_{22} , σ_{12} defined in the Cartesian coordinate system. The following basic equations of theory of elasticity hold:

- local equilibrium equations (involving Cauchy stress tensor)

$$\begin{cases} \frac{\partial \sigma_{11}}{\partial x_1} + \frac{\partial \sigma_{12}}{\partial x_2} + X_1 = 0 \\ \frac{\partial \sigma_{12}}{\partial x_1} + \frac{\partial \sigma_{22}}{\partial x_2} + X_2 = 0 \end{cases} \quad (1)$$

where X_1 and X_2 are body force components in x_1 and x_2 directions, respectively,

- the compatibility equation

$$\frac{\partial^2 \varepsilon_{11}}{\partial x_2^2} + \frac{\partial^2 \varepsilon_{22}}{\partial x_1^2} = \frac{2\partial^2 \varepsilon_{12}}{\partial x_1 \partial x_2} \quad (2)$$

where ε_{11} , ε_{22} , $\varepsilon_{12} = \frac{\gamma_{x_1 x_2}}{2}$ are strain components in the Cartesian coordinate system,

-Hook's law - linearly elastic stress-strain relations in plane stress

$$\begin{cases} \sigma_{11} = \frac{E}{1-\nu^2}(\varepsilon_{11} + \nu\varepsilon_{22}) \\ \sigma_{22} = \frac{E}{1-\nu^2}(\varepsilon_{22} + \nu\varepsilon_{11}) \\ \sigma_{12} = 2G\varepsilon_{12} \end{cases} \quad (3)$$

where E is the Young's modulus, G is the shear modulus and ν is the Poisson's ratio.

A possible solution strategy for a plane stress problem is the definition of the so-called Airy stress function

$$\begin{cases} \sigma_{11} = \frac{\partial^2 F}{\partial x_2^2} \\ \sigma_{22} = \frac{\partial^2 F}{\partial x_1^2} \\ \sigma_{12} = -\frac{\partial^2 F}{\partial x_1 \partial x_2} - x_1 X_2 - x_2 X_1 \end{cases} \quad (4)$$

This definition is compatible with local equilibrium equations (1). The equation (2) expressed in terms of F function leads to the biharmonic equation

$$\frac{\partial^4 F}{\partial x_1^4} + \frac{\partial^4 F}{\partial x_2^4} + 2 \frac{\partial^4 F}{\partial x_1^2 \partial x_2^2} = 0 \quad (5)$$

The methodology, reflected equation (5) is valid only for continuous, isotropic and homogeneous material fulfilling the Hooke's law. In the case of constant body forces X_1, X_2 the equation (5) is material-invariant (constants not affected by E, ν), and is also valid for plane strain cases.

The biharmonic equation (5) can be rewritten in polar coordinates (r, θ) as

$$\left(\frac{\partial^2}{\partial r^2} + \frac{1}{r} \frac{\partial}{\partial r} + \frac{1}{r^2} \frac{\partial^2}{\partial \theta^2} \right) \left(\frac{\partial^2 F}{\partial r^2} + \frac{1}{r} \frac{\partial F}{\partial r} + \frac{1}{r^2} \frac{\partial^2 F}{\partial \theta^2} \right) = 0 \quad (6)$$

where \bullet is $\left(\frac{\partial^2 F}{\partial r^2} + \frac{1}{r} \frac{\partial F}{\partial r} + \frac{1}{r^2} \frac{\partial^2 F}{\partial \theta^2} \right)$.

These initial considerations finally allow to formulate two main patterns describing the state of stress around the holes in thin plates. The first, simplified attempt was proposed by Girkmann [18], the second, more general, proposed by Howland [20].

ANALYTICAL SOLUTIONS

Let us consider a strip under tension with a circular hole, the stress state is described in polar coordinates (see Fig. 1). The circular hole is situated in the middle of the strip of the width $2b$, and the radius of the hole is a ($a < b$). Furthermore, a constant strip thickness $t = 1$ is assumed. The strip is subjected to tension under uniaxial load $p = const.$. The origin of the coordinate system is defined in the centre of the hole. In the analytical solutions [18], [20] the plate is infinitely thin and is made of isotropic, homogeneous and linearly elastic, Hookean material.

Girkmann's Solution

The Girkmann's solution [18] presents a large, thin plate containing a small circular hole is subjected to simple tension. The stress distribution is expressed by equations

$$\sigma_r = \frac{p}{2} \left(1 - \frac{a^2}{r^2} \right) - \frac{p}{2} \left(1 - \frac{4a^2}{r^2} + \frac{3a^4}{r^4} \right) \cos 2\theta \quad (7)$$



$$\sigma_{\theta} = \frac{p}{2} \left(1 + \frac{a^2}{r^2}\right) + \frac{p}{2} \left(1 + \frac{3a^4}{r^4}\right) \cos 2\theta \quad (8)$$

$$\sigma_{r\theta} = -\frac{p}{2} \left(1 + \frac{2a^2}{r^2} - \frac{3a^4}{r^4}\right) \sin 2\theta \quad (9)$$

where σ_r is the radial stress, σ_{θ} is the circumferential stress and $\sigma_{r\theta}$ is the shear stress.

TABLE 1. Coefficients d, e, l, m for $\lambda = 0.1$ and 0.5 .

λ	0.1	0.5
d_0	$5.01 \cdot 10^{-3}$	$1.32 \cdot 10^{-1}$
d_2	$2.54 \cdot 10^{-5}$	$2.33 \cdot 10^{-2}$
d_4	$3.15 \cdot 10^{-11}$	$3.14 \cdot 10^{-4}$
d_6	$1.40 \cdot 10^{-15}$	$7.51 \cdot 10^{-6}$
d_8	$5.00 \cdot 10^{-20}$	$1.45 \cdot 10^{-7}$
e_2	$-5.08 \cdot 10^{-3}$	$-1.89 \cdot 10^{-1}$
e_4	$-4.21 \cdot 10^{-9}$	$-1.70 \cdot 10^{-3}$
e_6	$-1.68 \cdot 10^{-13}$	$-3.64 \cdot 10^{-5}$
e_8	$-5.72 \cdot 10^{-18}$	$-6.70 \cdot 10^{-7}$
l_2	$4.13 \cdot 10^{-3}$	$1.40 \cdot 10^{-1}$
l_4	$1.06 \cdot 10^{-3}$	$3.27 \cdot 10^{-2}$
l_6	$2.83 \cdot 10^{-4}$	$8.09 \cdot 10^{-3}$
l_8	$7.24 \cdot 10^{-5}$	$1.95 \cdot 10^{-3}$
l_{10}	$1.82 \cdot 10^{-5}$	$4.71 \cdot 10^{-4}$
l_{12}	$4.65 \cdot 10^{-6}$	$1.14 \cdot 10^{-4}$
l_{14}	$1.15 \cdot 10^{-6}$	$2.80 \cdot 10^{-5}$
m_0	$5.69 \cdot 10^{-4}$	$1.40 \cdot 10^{-2}$
m_2	$-1.13 \cdot 10^{-3}$	$-3.62 \cdot 10^{-2}$
m_4	$-5.95 \cdot 10^{-4}$	$-1.78 \cdot 10^{-2}$
m_6	$-2.28 \cdot 10^{-4}$	$-6.47 \cdot 10^{-3}$
m_8	$-7.65 \cdot 10^{-5}$	$-2.08 \cdot 10^{-3}$
m_{10}	$-2.39 \cdot 10^{-5}$	$-6.30 \cdot 10^{-4}$
m_{12}	$-7.30 \cdot 10^{-6}$	$-1.84 \cdot 10^{-4}$

Howland's Solution

The problem of a plate with a circular hole is also addressed by R.C.J. Howland [20]. This solution assumes the strip is infinitely long.

In the analytical solution proposed by Howland, the stresses are expressed as follows

$$\sigma_r = p \left\{ \frac{1}{2} (1 - \cos 2\theta) + 2m_0 - \frac{d_0}{\rho^2} - 2 \sum_{n=1}^{\infty} \left[\frac{n(2n+1)d_{2n}}{\rho^{2n+2}} + \frac{(n+1)(2n-1)e_{2n}}{\rho^{2n}} + \dots \right. \right. \\ \left. \left. + n(2n-1)l_{2n}\rho^{2n-2} + (n-1)(2n+1)m_{2n}\rho^{2n} \right] \cos 2n\theta \right\} \quad (10)$$

$$\sigma_{\theta} = p \left\{ \frac{1}{2} (1 + \cos 2\theta) + 2m_0 + \frac{d_0}{\rho^2} + 2 \sum_{n=1}^{\infty} \left[\frac{n(2n+1)d_{2n}}{\rho^{2n+2}} + \frac{(n-1)(2n-1)e_{2n}}{\rho^{2n}} + \dots \right. \right. \\ \left. \left. + n(2n-1)l_{2n}\rho^{2n-2} + (n+1)(2n+1)m_{2n}\rho^{2n} \right] \cos 2n\theta \right\} \quad (11)$$

$$\sigma_{r\theta} = p \left\{ \frac{1}{2} \sin 2\theta + 2 \sum_{n=1}^{\infty} \left[n(2n-1) \left(l_{2n}\rho^{2n-2} - \frac{e_{2n}}{\rho^{2n}} \right) + n(2n+1) \left(m_{2n}\rho^{2n} - \frac{d_{2n}}{\rho^{2n+2}} \right) \right] \sin 2n\theta \right\} \quad (12)$$



where $\rho = r/b$ is the dimensionless coordinate, b is the strip half-width, n is the n -th expression of the series, e , d , l , m are the coefficients dependent on the ratio $\lambda = a/b$ and a is the hole radius.

The coefficients e , d , l , m are presented in the paper [20], computed for $\lambda \in \{0.1, 0.2, 0.3, 0.4, 0.5\}$. The selected coefficient values in the case of $\lambda = 0.1$ and $\lambda = 0.5$ are listed in Tab. 1.

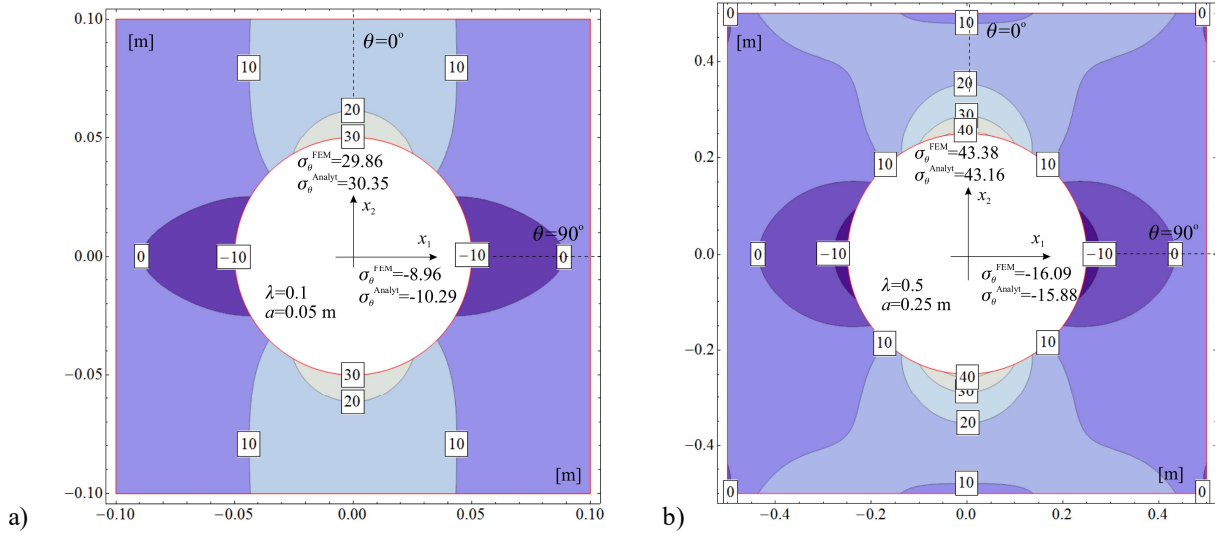


FIGURE 3. Howland's solution - contour lines of the circumferential stresses σ_θ [MPa] in the Cartesian coordinate system in the case of the hole with the radius a) $a = 0.05$ m and b) $a = 0.25$ m.

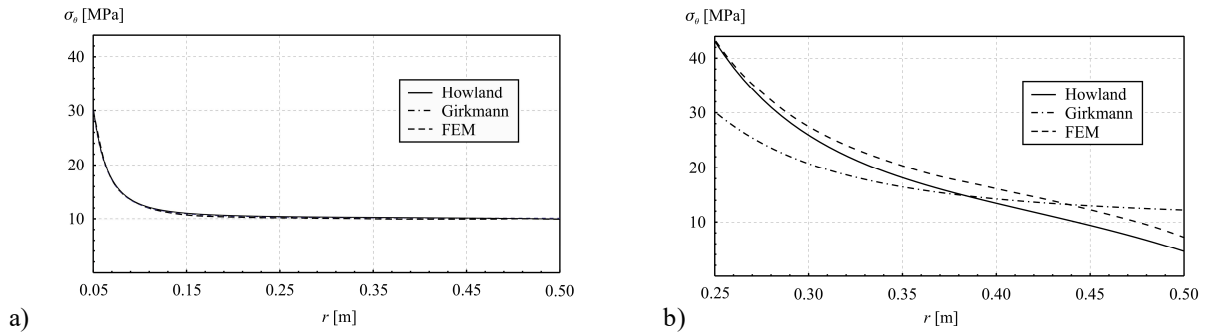


FIGURE 4. Circumferential stresses σ_θ [MPa] vs. radius r - distance of a given point from the centre of the hole for $\theta = 0^\circ$ for a) $a = 0.05$ m and b) $a = 0.25$ m.

NUMERICAL EXAMPLES – RESULTS AND CONCLUSIONS

Let us consider two strips of width $2b = 1$ m and thickness $t = 0.001$ m with holes of different diameters. The first case assumes the hole of the radius $a = 0.05$ m ($\lambda = a/b = 0.05/0.5 = 0.1$), the second case shows $a = 0.25$ m ($\lambda = a/b = 0.25/0.5 = 0.5$). It is assumed that the strips are subjected to axial load $p=q/t=10$ MN/m² which corresponds to the edge load $q = 10$ kN/m for $t = 0.001$ m.

In order to confirm the analytical results, numerical analysis has been performed by the FEM ABAQUS package [23]. The stresses were determined by a general static procedure. The applied FEM models are shown in Fig. 2. The strips are modelled by 3-node triangular general-purpose shell, finite membrane-strain elements type - S3. In both numerical examples the finite element mesh is subdivided around the holes. Material behaviour is modelled by a linearly elastic procedure available in the ABAQUS ($E = 210$ GPa, $\nu = 0.33$).

The major numerical results are shown in Figs. 3, 4 and in Tabs. 2, 3. The stresses are compared due to two analytical approaches [18], [20] and the FEM procedures.

Tab. 2 presents the stresses due to Howland's solution, in the section $\theta = 0^\circ$, in both cases $a = 0.05$ m and 0.25 m. The smaller hole case shows extreme circumferential stresses equal 30.348 MPa and for the larger hole case result is 43.158 MPa. In both cases the extreme stresses appear at the hole boundary. As the distance from the hole boundary increases, circumferential stresses decrease.

TABLE 2. Howland's solution - stresses [MPa] vs. radius r [m] - distance of a given point from the center of the hole for $\theta = 0^\circ$ for $a = 0.05$ m and 0.25 m.

r [m]	$a = 0.05$ m			$a = 0.25$ m		
	σ_r	σ_θ	$\sigma_{r\theta}$	σ_r	σ_θ	$\sigma_{r\theta}$
0.05	-0.001	30.348	0.00			
0.10	2.799	12.298	0.00			
0.15	1.430	10.837	0.00			
0.20	0.805	10.463	0.00			
0.25	0.484	10.309	0.00	0.081	43.158	0.00
0.30	0.295	10.225	0.00	3.732	27.447	0.00
0.35	0.172	10.108	0.00	3.278	20.386	0.00
0.40	0.086	10.098	0.00	1.964	16.097	0.00
0.45	0.026	10.014	0.00	0.685	12.394	0.00
0.50	-0.008	9.888	0.00	-0.151	8.018	0.00

TABLE 3. Howland's solution - stresses [MPa] vs. degree of θ [$^\circ$] for $r = a = 0.05$ m and $r = a = 0.25$ m.

θ [$^\circ$]	$r = a = 0.05$ m			$r = a = 0.25$ m		
	σ_r	σ_θ	$\sigma_{r\theta}$	σ_r	σ_θ	$\sigma_{r\theta}$
0	-0.001	30.348	0.00	0.081	43.158	0.00
15	-0.001	27.623	0.001	0.066	37.241	0.008
30	0.00	20.180	0.002	0.031	23.125	0.010
45	0.001	10.016	0.002	-0.007	7.570	0.008
60	0.003	-0.142	0.002	-0.039	-5.084	0.005
75	0.004	-7.575	0.001	-0.059	-13.131	0.002
90	0.004	-10.295	0.00	-0.065	-15.880	0.00

In the considered section $\theta=0^\circ$, the maximum radial stresses are 2.799 MPa at a distance 0.05 m from the hole boundary in the small hole case (see Tab. 2). In the case of bigger hole the maximum radial stress is 3.732 MPa at the same distance 0.05 m from the hole edge (see Tab. 2). Shear stresses in both cases are zero. Tab. 3 presents stress variation on the hole boundary in the function of θ . The circumferential stresses are extreme on the edge of the hole. Radial and shear stresses at the entire edge of the hole tend to zero. Figs. 3 and 4 present circumferential stresses. Fig. 3 shows the contours of circumferential stresses in the Cartesian coordinate system. Fig. 4 shows circumferential stresses for $\theta = 0^\circ$ only. Due to both hole sizes, the circumferential stresses curves indicate a local stress concentration at the edges hole boundaries. Fig. 4 compares the analytical results due to Girkmann's and Howland's solutions with the FEM its assumption. In the small hole case ($\lambda = 0.1$, $a = 0.05$ m), all three approaches converge. However, in the larger hole area the Girkmann's solution, due its assumption significantly differs from the Howland's proposal results and the FEM solution.

Comparison of the analytical solutions with the FEM solutions leads to the conclusion that the Howland's version [20] is dedicated to stress analysis around circular holes in all the proportions of hole areas to the strips/plates areas. On the other hand the Girkmann's solution [18], is limited only to the cases of the hole area significantly smaller than the plate area (see Fig. 4).

ACKNOWLEDGMENTS

The calculation presented in the paper were carried out at the TASK Academic Computer Centre in Gdansk, Poland.

REFERENCES

1. W. Tseng and J. Tarn, *Journal of Mechanics* **30**, 611-624 (2014).
2. A. Abuzaid, M. Hrairi, and M. S. Dawood, *IOP Conference Series: Materials Science and Engineering* **184** (2017).
3. R. Dimitri, N. Fantuzzi, F. Tornabene, and G. Zavarise, *International Journal of Mechanical Sciences* **118**, 166-187 (2016).
4. I. Khoma and O. Dashko, *International Applied Mechanics* **52**, 605-615 (2016).
5. M. Jafari and E. Ardalani, *International Journal of Mechanical Sciences* **106**, 220-230 (2016).
6. Y. Zheng, "The interaction of holes on stress and strain concentrations in uniaxially loaded tensile plates," in *Materials, Mechanical Engineering and Manufacture* (2013).
7. N. Bojic and Z. Jugovic, "Stress concentration in plates with one hole," in *Sixth International Symposium about Forming and Design in Mechanical Engineering* (2010), pp. 73-78.
8. V. Vasil'ev and L. Fedorov, *Mechanics of Solids* **43**, 528-538 (2008).
9. J. Kang, *International Journal of Mechanical Sciences* **89**, 482-486 (2014).
10. S. Akbarov and N. Yahnioglu, *Mechanics of Composite Materials* **44**, 581-590 (2008).
11. N. Odishelidze, F. Criado-Aldeanueva, F. Criado, and J. Sanchez, *Mathematics and Mechanics of Solids* (2016).
12. Z. Yang, C. Kim, C. Cho, H. Beom, and S. Song, "The size effect on the concentration of stress and strain in finite thickness elastic plate containing a circular hole," in *Engineering structural integrity research development and application* (2007), pp. 758-761.
13. Z. Yang, C. Kim, C. Cho, and H. Beom, *International Journal of Solids and Structures* **45**, 713-731 (2008).
14. Z. Yang, *International Journal of Fracture* **155**, 43-54 (2009).
15. Z. Yang, J. Hou, G. Wang, and Z. Xiong, "The stress and strain concentrations associated with two interacting holes in a finite thickness elastic plate subjected to tensile stress," in *Fracture and Strength of Solids* (2011).
16. S. Wang, A. Lu, X. Zhang, and N. Zhang, *Mechanics based design of structures and machines* **46**, 23-37 (2018).
17. V. Sokolov, D. Strachov, and L. Sinyakov, *Magazine of Civil Engineering* **70**, 33-41 (2017).
18. K. Girkmann, *Shell structures*, (in Polish) (ARKADY, 1957).
19. A. Ugural and S. Fenster, *Advanced strength and applied elasticity* (Prentice Hall, 2003).
20. R. Howland, *On the stresses in the neighborhood of a circular hole in a strip under tension* (Royal Society of London, 1930).
21. G. Savin, *Stress distribution around holes* (National Aeronautics and Space Administration, 1968).
22. A. Love, *A treatise on the mathematical theory of elasticity* (Cambridge University Press, 2013).
23. D. Hibbit, B. Karlsson, and P. Sorensen, *ABAQUS analysis user's manual* (Hibbit, Karlsson, Sorensen Inc.).